

# Resveratrol-decreased hyperalgesia mediated by the P2X<sub>7</sub> receptor in gp120-treated rats

Bing Wu<sup>1\*</sup>, Yucheng Ma<sup>2\*</sup>, Zhihua Yi<sup>1</sup>, Shuangmei Liu<sup>1</sup>, Shenqiang Rao<sup>1</sup>, Lifang Zou<sup>1</sup>, Shouyu Wang<sup>1</sup>, Yun Xue<sup>1</sup>, Tianyu Jia<sup>1</sup>, Shanhong Zhao<sup>1</sup>, Liran Shi<sup>1</sup>, Lin Li<sup>1</sup>, Huilong Yuan<sup>1</sup> and Shangdong Liang<sup>1</sup>

## Abstract

**Background:** Chronic pain is a common symptom in human immunodeficiency virus (HIV)-1 infection/acquired immunodeficiency syndrome patients. The literature shows that the HIV envelope glycoprotein 120 (gp120) can directly cause hyperalgesia by stimulating primary sensory afferent nerves. The P2X<sub>7</sub> receptor in the dorsal root ganglia (DRG) is closely related to neuropathic and inflammatory pain. In this study, we aimed to explore the effect of resveratrol (RES) on gp120-induced neuropathic pain that is mediated by the P2X<sub>7</sub> receptor in the rat DRG.

**Results:** Mechanical hyperalgesia in rats treated with gp120 was increased compared with that in the sham group. The P2X<sub>7</sub> expression levels in rats treated with gp120 were higher than those in the sham group. Co-localization of the P2X<sub>7</sub> receptor and glial fibrillary acidic protein (GFAP, a marker of satellite glial cells [SGCs]) in the DRG SGCs of the gp120 group exhibited more intense staining than that of the sham group. RES decreased the mechanical hyperalgesia and P2X<sub>7</sub> expression levels in gp120 treatment rats. Co-localization of the P2X<sub>7</sub> receptor and GFAP in the gp120+ RES group was significantly decreased compared to the gp120 group. RES decreased the IL-1 $\beta$  and TNF- $\alpha$  receptor (R) expression levels and ERK1/2 phosphorylation levels as well as increased IL-10 expression in the DRG of gp120-treated rats. Whole cell clamping demonstrated that RES significantly inhibited adenosine triphosphate-activated currents in HEK293 cells that were transfected with the P2X<sub>7</sub> plasmid.

**Conclusions:** RES relieved mechanical hyperalgesia in gp120-treated rats by inhibiting the P2X<sub>7</sub> receptor.

## Keywords

HIV gp120-associated neuropathic pain, P2X<sub>7</sub> receptor, resveratrol, dorsal root ganglia

Date received: 16 September 2016; revised: 24 March 2017; accepted: 2 April 2017

## Introduction

Chronic pain is a common symptom in human immunodeficiency virus (HIV)-1 infection/acquired immunodeficiency syndrome (AIDS) patients.<sup>1–3</sup> The quality of life of HIV-1/AIDS patients with chronic pain is significantly decreased. To ascertain the pathogenic mechanism of HIV-associated pain, it is pivotal to identify the causative HIV-1 agents. Glycoprotein 120 (gp120) can cause axonal injury of sensory neurons in culture.<sup>4,5</sup> Gp120 is an HIV-1 protein that induces pain behaviors when introduced into animal models.<sup>1,5–8</sup> Pain may arise from the direct effects of HIV on the peripheral nervous system.<sup>4,9</sup> The dorsal root ganglion (DRG) afferent fibers are distributed to

both central and peripheral terminals and they transmit noxious stimuli from the periphery to the central nervous system.<sup>10,11</sup> Gp120 appears to bind to the surface of rat

<sup>1</sup>Department of Physiology, Medical College of Nanchang University, Nanchang, Jiangxi, People's Republic of China

<sup>2</sup>Queen Mary School, Medical College of Nanchang University Nanchang, Jiangxi, People's Republic of China

\*Bing Wu and Yucheng Ma contributed equally to this work.

## Corresponding author:

Shangdong Liang, Department of Physiology, Medical School of Nanchang University, Nanchang, Jiangxi 330006, P.R. China.  
Email: liangsd@hotmail.com



DRG neurons and may be causative factors in the generation of neuropathic pain in HIV-1-infected patients.<sup>10,12</sup> The HIV-1 gp120 level was significantly higher in “pain-positive” HIV-1 patients.<sup>4,5</sup> Therefore, preventing and treating HIV-1 gp120-associated neuropathic pain has become a heavily researched subject.

Resveratrol (RES) is a natural polyphenolic compound found in peanuts, mulberries, grapes, and red wine.<sup>13,14</sup> RES exhibits anti-inflammatory and anti-nociceptive effects.<sup>13–15</sup> Adenosine triphosphate (ATP) is a signaling molecule in neuropathic and inflammatory pain.<sup>16–18</sup> Extracellular ATP can activate the ionotropic P2X receptors in primary afferent fibers.<sup>16–18</sup> The P2X<sub>7</sub> receptor is involved in the induction and maintenance of neuropathic and inflammatory pain.<sup>17,19,20</sup> The interaction between HIV-1 gp120 and macrophages stimulates increased ATP release and P2X receptors activated by ATP are required for HIV entry into macrophages.<sup>21,22</sup> ATP signaling via the P2X<sub>7</sub> receptor is related to the regulation of inflammatory responses during acute viral infection.<sup>22</sup> The blocking of purinergic receptors results in a significant reduction in the HIV replication in macrophages.<sup>21</sup> Therefore, the P2X<sub>7</sub> receptor may be involved in HIV-associated neuropathic pain. In this study, we investigated the effect of RES on gp120-induced neuropathic pain mediated by the P2X<sub>7</sub> receptor in rat DRGs.

## Materials and methods

### Animals and surgical methods

Adult (200–250 g) male Sprague–Dawley (SD) rats were used in all experiments and housed with an alternating 12-h light/dark cycle. They were provided with food and water *ad libitum*. The use of the animals was reviewed and approved by the Animal Care and Use Committee of Medical College of Nanchang University. The experiments were conducted under the guidelines of the NIH in the US regarding the care and use of animals for experimental procedures.

The rats were randomly divided into the following three groups (with six rats in each group): the HIV-gp120 group (gp120 group); HIV-gp120 rats treated with RES group (gp120 + RES group); and sham operation group (sham group). A previously described technique<sup>23</sup> was used for the perineural HIV-gp120 administration. Briefly, under 10% chloral hydrate anesthesia (3 ml/kg, *i.p.*, supplemented as necessary) and aseptic surgical conditions, the left sciatic nerve of the SD rats was exposed in the popliteal fossa without damaging the nerve construction. A 2 × 6 mm strip of oxidized regenerated cellulose was previously soaked in 250 µl of a 0.1% rat serum albumin saline solution containing 200 ng of gp120 (Sigma) or 0.1% rat serum albumin in

saline for the sham surgery. A 3–4 mm length of the sciatic nerve that was proximal to the trifurcation was wrapped loosely with the soaked cellulose, did not cause nerve constriction, and was left *in situ*. The incision was closed with 4/0 sutures. Beginning at 24 h after surgery, the rats in the gp120 + RES group were intraperitoneally treated with RES (30 mg/kg) daily for 14 days.<sup>24</sup> Rats in the sham and gp120 groups were intraperitoneally injected with the same volume of normal saline.

### Measurement of the mechanical withdrawal threshold

Determination of the mechanical withdrawal threshold (MWT) was performed at 9:00–12:00 using a BME-404 electronic mechanical stimulator (Institute of Biomedical Engineering, Chinese Academy of Medical Sciences, Tianjin, China). The main technical parameters of this equipment were as follows: end face diameter of the test needle, 0.6 mm; pressure measurement range, 0.1–50 g; and pressure measurement resolution, 0.05 g. An organic glass box (22 × 22 × 12 cm) was placed on the sieve of the metal frame. The rat was placed into the box for 30 min of adaptation. The left hind paws were touched with the test needle until escaping behavior was observed. The pressure value was automatically recorded. The measurement was conducted five times for each rat (interval, ≥ 5 min), and the mean value was calculated as the MWT for this measurement.<sup>7,25,26</sup>

### RNA extraction and Real-time-PCR

The rats in three groups were anesthetized using 10% chloral hydrate (3 ml/kg, *i.p.*). The L4–6 DRGs were isolated immediately and flushed with ice-cold phosphate-buffered saline (PBS). The total RNA samples were prepared from the L4–6 DRGs of each group using the TRIzol Total RNA Reagent (Beijing Tiangen Biotech Co.). cDNA synthesis was performed with 2 µg of total RNA using a RevertAid™ H Minus First Strand cDNA Synthesis Kit (Fermentas, Burlington, Ontario, Canada). The primers were designed with Primer Express 3.0 software (Applied Biosystems), and the sequences were as follows: P2X<sub>7</sub>, forward 5'-CTTCGGCGTGCCTTTTG-3', and reverse 5'-AGGACAGGGTGGATCCAATG-3' as well as β-actin, forward 5'-TAAAGACCTCTATGCCAACACAGT-3', and reverse 5'-CACGATGGAGGGGCCGACTCATC-3'. Quantitative PCR was performed using the SYBR® Green MasterMix in an ABI PRISM® 7500 Sequence Detection System (Applied Biosystems, Inc.: Foster City, CA). The quantification of gene expression was performed using the ΔΔCT calculation with CT as the threshold cycle. The relative levels of target genes, normalized to the sample with the lowest CT, are given

as  $2^{-\Delta\Delta CT}$ .<sup>27</sup>  $\beta$ -actin was used to be internal control in the three groups. The relative expression levels of mRNA in the three groups were normalized to  $\beta$ -actin.

### Western blot analysis

The animals were anesthetized and tissue collection was performed as described above, except that the tissues were snap-frozen in tubes on dry ice during collection.<sup>25</sup> Briefly, on the 14th day after the operation, the animals were anesthetized with 10% chloral hydrate and L4-6 DRGs were isolated immediately and rinsed in ice-cold PBS. The ganglia were homogenized by mechanical disruption in lysis buffer containing the following: 50 mM Tris-Cl, pH 8.0, 150 mM NaCl, 0.1% sodium dodecyl sulfate (SDS), 1% Nonidet P-40, 0.02% sodium deoxycholate, 100  $\mu$ g/mL phenylmethylsulfonyl fluoride, and 1  $\mu$ g/mL Aprotinin. The cells were incubated on ice for 30 min. The homogenates were then centrifuged at 12,000 r/min for 10 min and the supernatants were collected. The quantity of total proteins in the supernatants was determined using the Lowry method. After dilution with loading buffer (250 mM Tris-Cl, 200 mM Dithiothreitol, 10% SDS, 0.5% Bromophenol Blue, and 50% Glycerol) and heating to 95°C for 5 min, samples containing equal protein levels (20  $\mu$ g) were separated by 10% SDS-polyacrylamide gel electrophoresis with a Bio-Rad system. The proteins were then transferred onto polyvinylidene difluoride membranes by electrophoretic transfer using the same system. The membrane was blocked with 5% bovine serum albumin (BSA) for anti-p-ERK1/2 and anti-ERK1/2 in 25 mM tris-buffered saline, pH 7.2, plus 0.05% Tween 20 (TBST) for 2 h at room temperature, which was followed by incubation with a rabbit anti-P2X<sub>7</sub> (1:800 dilutions, Abcam, USA), rabbit anti-TNF $\alpha$ -receptor (R), rabbit anti-IL-1 $\beta$  and rabbit anti IL-10 (1:500 dilutions, Abcam, USA), rabbit anti-p-ERK1/2 (Thr202/Tyr204) (1:1000, Cell signaling technology, 9101), rabbit anti-ERK1/2 (1:1000, Cell signaling technology, 9102), and mouse monoclonal anti- $\beta$ -actin antibody (1:800 dilutions, Beijing Zhongshan Biotech Co., China) at 4°C overnight. The membranes were washed three times with TBST and incubated (1 h, room temperature) with a horseradish peroxidase-conjugated secondary antibody (goat anti-rabbit IgG (1:2000), goat anti-mouse IgG (1:2000), Beijing Zhongshan Biotech Co.) in blocking buffer. After another wash cycle, the labeled proteins were visualized by enhanced chemiluminescence on a high-performance film (Shanghai Pufei Biotech Co.). The chemiluminescent signals were collected on an autoradiography film, and the band intensity was quantified using Image Pro Plus software. The relative band intensity of the target proteins was normalized against the intensity of the respective  $\beta$ -actin internal control.

### Double immunofluorescence

The DRGs isolated from rats in the three groups, six rats in each group, were washed with PBS. The DRGs were dissected immediately and fixed in 4% paraformaldehyde for 24 h at room temperature. Then, they were transferred to 20% sucrose for dehydration at 4°C overnight. The tissues were sectioned at 10  $\mu$ m using a cryostat and placed onto glass slides that were coated with poly-d-lysine for storage in the refrigerator at -20°C. After washing with PBS three times, the preparations were preincubated with 10% normal goat serum (Jackson ImmunoResearch Inc., West Grove PA, USA) for 40 min in a moist chamber at 37°C. The sections were then incubated with chicken anti-GFAP (1:1000 dilutions; Abcam, USA) and rabbit anti-P2X<sub>7</sub> (1:200 dilutions; Abcam, USA), which were diluted in PBS, overnight at 4°C. After three rinses in PBS, the sections were then incubated with fluorescent goat anti-chicken fluorescein isothiocyanate (FITC) and goat anti-rabbit tetramethylrhodamine isothiocyanate (TRITC) secondary antibodies (1:200 dilutions for both secondary antibodies; Jackson ImmunoResearch, PA, USA) in the dark at 37°C for 40 min. The prepared sections were washed three times in PBS before they were mounted in glycerol and cover slipped. After these steps, the sections were examined using fluorescence microscopy. Image-Pro Plus 6.0 image analysis software (Media Cybernetics Inc.) was used to quantify the co-localization of GFAP and P2X<sub>7</sub>. To specify the immunoreactivity of GFAP and P2X<sub>7</sub>, normal goat serum and PBS were used as negative controls in place of the primary antibodies.

### HEK 293 cell culture and transfection

HEK 293 cells were grown in Dulbecco's modified Eagle's medium supplemented with 10% fetal bovine serum, 1% penicillin, and streptomycin at 37°C in a humidified atmosphere containing 5% CO<sub>2</sub>. Cells were transiently transfected with the human pcDNA3.0-EGFP-P2X<sub>7</sub> plasmid using Lipofectamine 2000 reagent (Invitrogen) according to the manufacturer's instructions. The Genbank accession number is NM\_019256.1. The hP2X<sub>7</sub>R plasmid was purchased from Shanghai Genaray Biotech Co., Ltd. When HEK293 cells were 70%–80% confluent, cell culture media was replaced with OptiMEM 2 h before transfection. The transfection media were prepared as follows: (a) 4  $\mu$ g DNA was diluted into a 250  $\mu$ l final volume of OptiMEM, (b) 10  $\mu$ l Lipofectamine2000 was diluted into a 250  $\mu$ l final volume of OptiMEM, and (c) the Lipofectamine-containing solution was mixed with the plasmid-containing solutions, which was incubated at room temperature (RT) for 20 min. Subsequently, 500  $\mu$ l of cDNA/lipofectamine solution was added to each well. Cells were incubated for 6 h at 37°C in 5% CO<sub>2</sub>. After incubation, the cells were

washed in MEM containing 10% FBS and incubated for 24–48 h. The green fluorescent protein (GFP) fluorescence was assessed as a reporter for the efficiency of transfection. Whole-cell patch clamp recordings were performed one to two days after transfection.

### Electrophysiological recordings

The electrophysiological recording was performed using a patch/whole cell clamp amplifier (Axopatch 200B).<sup>28</sup> The micropipette was filled with internal solution (in mM) containing KCl 140, MgCl<sub>2</sub> 2, HEPES 10, EGTA 11, and ATP 5. The osmolarity was adjusted to 340 mOsm/kg with sucrose and pH was adjusted to 7.4 with KOH. The external solution (in mM) contained NaCl 150, KCl 5, CaCl<sub>2</sub> 2.5, MgCl<sub>2</sub> 1, HEPES 10, and D-glucose 10. Its osmolarity was adjusted to 340 mOsm with sucrose and pH was adjusted to 7.4 with NaOH. The resistance of recording electrodes was in the range of 1–4 MΩ; 3 MΩ was the best. A small patch of membrane underneath the pipette tip was aspirated to form a seal (1–10 GΩ). Then, a more negative pressure was applied to rupture it and establish a whole-cell mode. The holding potential was set at –60 mV. The drugs were dissolved in an external solution and delivered by gravity flow from an array of tubules (500 μm O.D. and 200 μm I.D.) connected to a series of independent reservoirs. The distance from the tubule mouth to the examined cell was approximately 100 μm. Rapid solution exchange was achieved by horizontally shifting the tubules with a micromanipulator.

### Statistical analysis

The data were analyzed using SPSS 20 software. The numerical values were reported as the mean ± SEM. Statistical significance was determined by one-way analysis of variance followed by the Fisher's post hoc test for multiple comparisons. A p-value < 0.05 was considered statistically significant.

## Results

### Effects of RES on hyperalgesia in gp120-treated rats

Mechanical hyperalgesia was tested with a mechanical stimulator. There was no difference in the MWT between the gp120 and sham groups before the operation ( $p > 0.05$ ). At 4 to 14 days after the operation, the MWT in the gp120 group was lower than the sham group ( $p < 0.05$ ) and there was a significant difference from days 7 to 14 ( $p < 0.01$ ). The MWT in the gp120 + RES group was higher than the gp120 group from days 4 to 14 ( $p < 0.05$ ), and there was a significant difference from days 12 to 14 ( $p < 0.01$ ) (Figure 1).

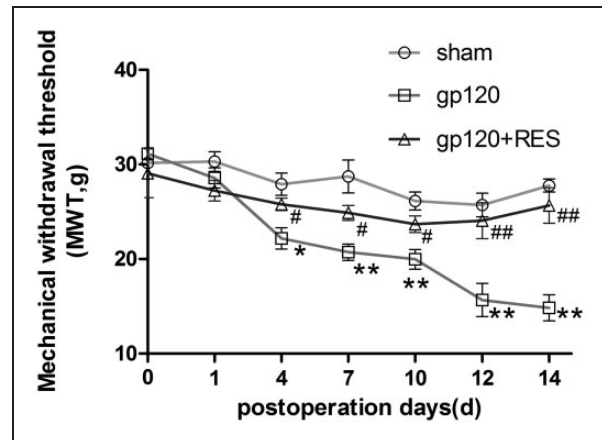


**Figure 1.** Effects of RES on the mechanical withdrawal threshold (MWT) in gp120-treated rats. Each group consisted of six rats ( $n = 6$  per group). The data represent the mean ± SEM. The significant differences are noted as “\*” for  $p < 0.05$  and “\*\*” for  $p < 0.01$  compared to the sham group; significant differences are denoted as “#” for  $p < 0.05$  and “##” for  $p < 0.01$  compared to the gp120-treated group.

### Effects of RES on the expression of the P2X<sub>7</sub> mRNA and protein in the DRG of the gp120-treated rats

The expression of the P2X<sub>7</sub> mRNA in the DRG was measured by RT-PCR. The relative levels of the P2X<sub>7</sub> mRNA in the gp120 group were significantly increased compared to the sham group ( $p < 0.01$ ). The expression levels of the P2X<sub>7</sub> mRNA in the gp120 + RES group were significantly decreased compared to the gp120 group ( $p < 0.01$ ) (Figure 2(a)).

The expression levels of the P2X<sub>7</sub> protein in the DRG were analyzed by Western blot analysis. Using image analysis, the P2X<sub>7</sub> protein expression (normalized to each β-actin in the internal control) in the gp120 group was significantly enhanced compared to the sham group ( $p < 0.01$ ). The relative levels of the P2X<sub>7</sub> protein expression in the gp120 + RES group were lower than the gp120 group ( $p < 0.01$ ) (Figure 2(b)).

### Effects of RES on the co-localization of P2X<sub>7</sub> and GFAP by double immunofluorescence in the DRGs of the gp120-treated rats

The co-localization of the P2X<sub>7</sub> receptor and GFAP (a marker of SGCs) was measured by double immunofluorescence. The upregulated expression of GFAP was a typical characteristic of active SGCs. The immunofluorescence results showed that the P2X<sub>7</sub> receptor and GFAP were co-localized in the DRG SGCs. The co-localization of the P2X<sub>7</sub> receptor and GFAP in the gp120 group exhibited more intense staining than the sham group. The co-localization of the P2X<sub>7</sub> receptor

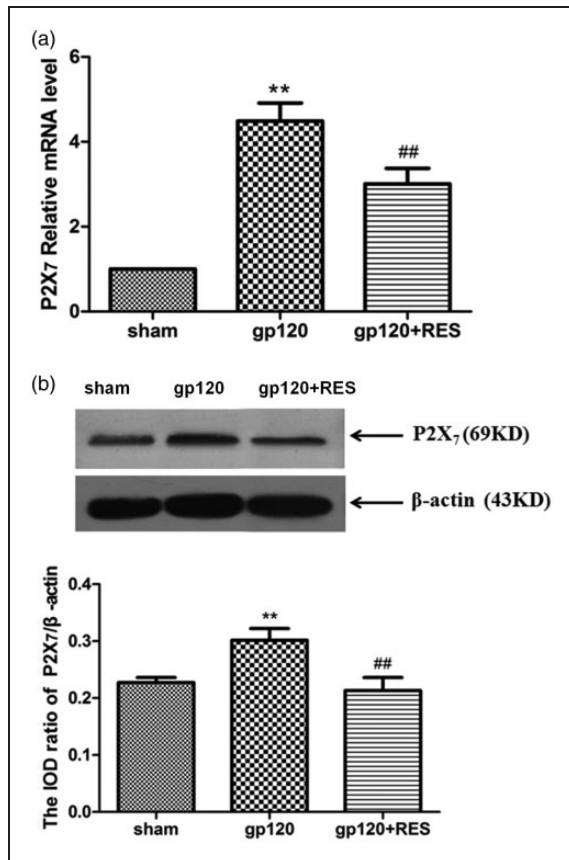


**Figure 2.** Effects of RES on the expression of P2X<sub>7</sub> mRNA and protein in L4–6 DRGs from each group. (a) The P2X<sub>7</sub> mRNA expression level in the DRG of the gp120 group was increased compared to the sham group ( $p < 0.01$ ). The P2X<sub>7</sub> mRNA level in the DRG of the gp120 + RES group was decreased compared to the gp120 group ( $p < 0.01$ ). The experiment was performed in triplicate and repeated three times.  $\beta$ -actin was an internal control to normalize the mRNA expression level of the three groups to different amounts of tissue. And the expression levels of each group were normalized to the sham group. The data represent the mean  $\pm$  SEM. \*\* $p < 0.01$ , compared to the sham group and ## $p < 0.01$ , compared to the gp120-treated group. (b) The expression of P2X<sub>7</sub> protein in the DRG of the gp120-treated group was increased compared to the sham group ( $p < 0.01$ ). The P2X<sub>7</sub> protein expression in the DRG of the gp120 + RES group was decreased compared to the gp120 group ( $p < 0.01$ ). The bar histograms show the ratio of the P2X<sub>7</sub> protein level to the  $\beta$ -actin level in each group (Note: The data are shown as the mean  $\pm$  SEM. \*\* $p < 0.01$ , compared to the sham group and ## $p < 0.01$ , compared to the gp120 group).

and GFAP in the gp120 + RES group was significantly decreased compared to the gp120 group (Figure 3).

#### Effects of RES on the expression of TNF $\alpha$ -R, IL-1 $\beta$ , and IL-10 proteins in the DRG of gp120-treated rats

The expression levels of TNF $\alpha$ -R, IL-1 $\beta$ , and IL-10 proteins in the DRG were analyzed by Western blot

analysis. Using image analysis, the values for the TNF $\alpha$ -R and IL-1 $\beta$  protein expression levels (normalized to each  $\beta$ -actin internal control) in the gp120 group were significantly augmented compared to the sham group ( $p < 0.01$ ). The relative values of the TNF $\alpha$ -R and IL-1 $\beta$  protein expression levels in the gp120 + RES group were lower than the gp120 group ( $p < 0.01$ ) (Figure 4).

The IL-10 protein expression levels in the gp120 group were decreased compared to the sham group ( $p < 0.01$ ). The IL-10 protein expression levels in the gp120 + RES group were increased compared to the gp120 group ( $p < 0.01$ ) (Figure 4).

#### Effects of RES on the ERK1/2 and p-ERK1/2 expression levels in the DRG of gp120-treated rats

The phosphorylation and activation of ERK1/2 are involved in inflammatory pain. The ERK1/2 and p-ERK1/2 expression levels in the DRG were analyzed by Western blot analysis. The integrated optical density (IOD) ratio of p-ERK1/2 to ERK1/2 was higher in the gp120 group than in the sham group ( $p < 0.01$ ,  $n = 6$  for each group). The results indicated that the role of extracellular signal-regulated protein kinase (ERK) phosphorylation in the DRG is related to the P2X<sub>7</sub> receptor-mediated hyperalgesia in the gp120-treated rats.

In addition, we examined whether the administration of RES was able to affect the phosphorylation of ERK in the gp120 group DRG. The IOD ratio of p-ERK1/2 to ERK1/2 in the gp120 + RES group was significantly lower than the gp120 group ( $p < 0.01$ ,  $n = 6$  for each group) (Figure 5). These results suggest that the RES effects on the P2X<sub>7</sub> receptor-mediated hyperalgesia may help decrease the ERK1/2 phosphorylation and activation in the DRG of the gp120-treated rats.

#### Depressive effects of RES on ATP-induced current in HEK293 cells expressing the hP2X<sub>7</sub> receptor

The ATP-activated currents in HEK293 cells transfected with pEGFP-hP2X<sub>7</sub> plasmid were recorded by whole cell patch clamping. The ATP-activated currents in HEK293 cells can be inhibited by RES (Figure 6(a)). The concentration dependence of ATP on the peak amplitude of current responses by the P2X<sub>7</sub> receptor in the absence (closed symbols) and presence of RES (100  $\mu$ M) (open symbols) ( $p < 0.05$ ,  $n = 8-10$ ) was showed in Figure 6(b).

## Discussion

Elucidation of how HIV-1 infection causes chronic pain is essential for developing effective therapy. HIV-1 gp120, as a potential pathogenically relevant factor, is involved in neuropathic pain.<sup>1,5,8</sup> Our data showed that the MWT in the peripheral gp120-treated rats was

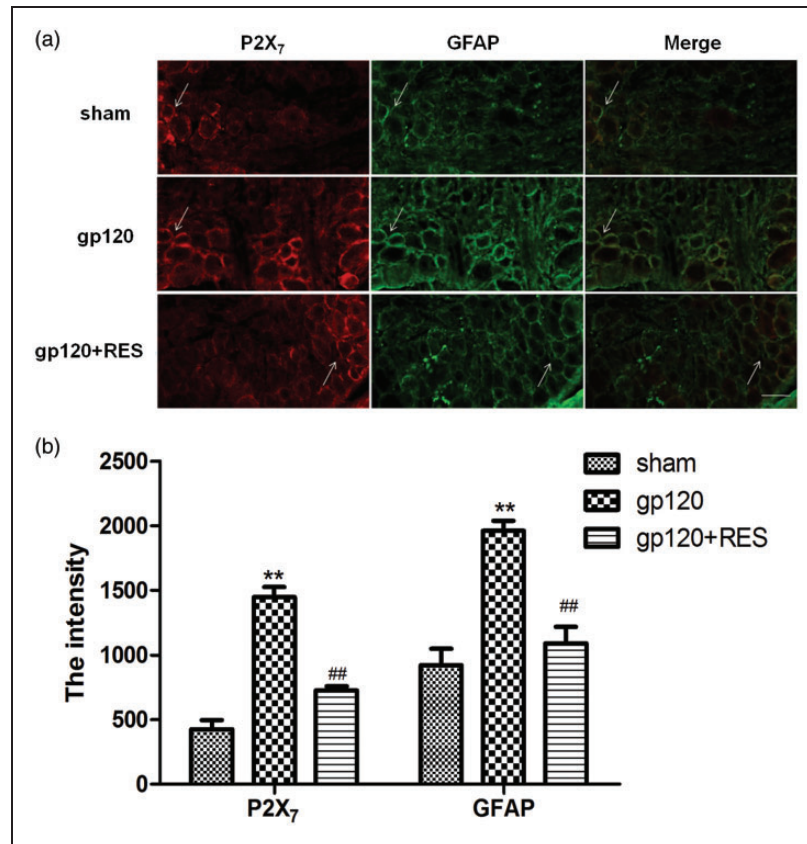


**Figure 3.** Double immunostaining for GFAP and the P2X<sub>7</sub> receptor in the DRG. (a) GFAP and P2X<sub>7</sub> immunoreactivity levels were analyzed in DRG sections. Double labeling for GFAP and P2X<sub>7</sub> in a single section of the DRG. The green signal represents GFAP staining with a FITC-conjugated secondary antibody, and the red signal indicates P2X<sub>7</sub> staining with a TRITC-conjugated secondary antibody. The scale bars denote 100  $\mu$ m. (b) Quantification of P2X<sub>7</sub> (red) and GFAP (green). The GFAP and P2X<sub>7</sub> intensity of the immunoreactivity in the gp120 group were increased compared to the sham group ( $p < 0.01$ ,  $n = 6$ ). The GFAP and P2X<sub>7</sub> intensity in the gp120 + RES group were decreased compared to the gp120 group ( $p < 0.01$ ,  $n = 6$ ). Data presented as means  $\pm$  SEM. \*\* $p < 0.01$ , compared to sham group, and ## $p < 0.01$ , compared to gp120 group.

decreased compared to the sham rats, which was consistent with previous reports.<sup>8,23,29</sup> The DRG can transmit pain signals from the periphery to the central nervous system.<sup>10,11</sup> The P2X<sub>7</sub> receptor in the DRG is related to inflammatory and neuropathic pain.<sup>17,19,20,30</sup> Our study demonstrated that the P2X<sub>7</sub> mRNA and protein levels in the HIV-1 gp120-treated rats were significantly enhanced compared with those in the sham rats. The increased P2X<sub>7</sub> receptor in the DRG may be involved in HIV-associated neuropathic pain. After treatment with RES, the P2X<sub>7</sub> receptor mRNA and protein levels were decreased. Meanwhile, the MWT in the gp120 + RES group was higher than that in the gp120 group. Our results indicated that RES might decrease the upregulated expression of the P2X<sub>7</sub> receptor and inhibit the transmission of nociceptive signaling. This effect may eventually alleviate the HIV-associated pain behavior in the gp120 group rats.

The SGCs envelop the neuronal soma in the DRG.<sup>31</sup> Double immunohistochemical staining showed that co-

localization of the P2X<sub>7</sub> receptor and GFAP in the DRG in the gp120-treatment rats was increased. GFAP is a marker of SGCs.<sup>32</sup> Our data indicated that the expression of the P2X<sub>7</sub> receptor in the DRG SGCs was increased. The GFAP upregulation in the DRG SGCs of gp120 treatment rats indicates the activation of SGCs.<sup>32,33</sup> The activation of SGCs can release cytokines and thus augment neuronal excitation.<sup>31,32</sup> The results showed that the TNF $\alpha$ -R and IL-1 $\beta$  protein levels in the gp120 group were significantly increased compared to the sham group, and the IL-10 protein levels (anti-inflammatory factor) in the gp120 group were decreased compared to the sham group. RES inhibited the increased expression levels of P2X<sub>7</sub> and GFAP in the DRG SGCs. After the gp120 rats were treated with RES, the relative TNF $\alpha$ -R and IL-1 $\beta$  protein levels were lower than the gp120 rats and the IL-10 protein levels were increased compared to the gp120 rats. RES may inhibit the upregulated P2X<sub>7</sub> and GFAP levels in the DRG and decrease the activation of SGCs. RES may

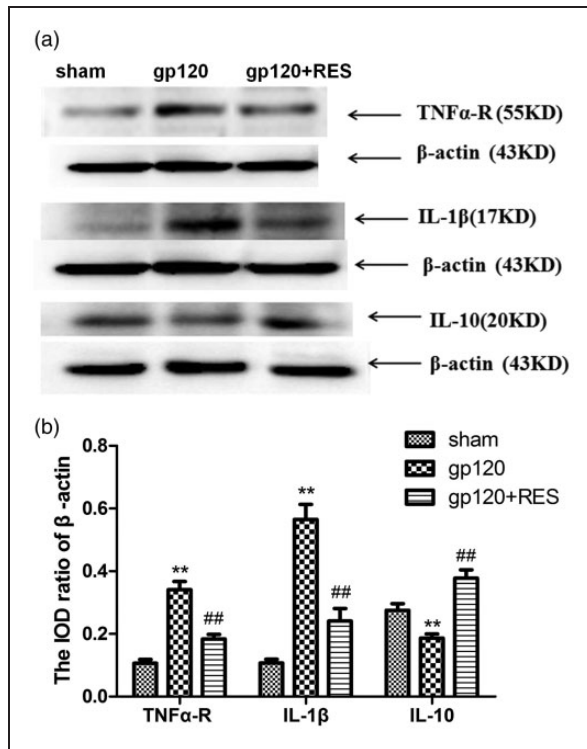


**Figure 4.** Effects of RES on the TNF $\alpha$ -R, IL-1 $\beta$ , and IL-10 protein expression levels in L4–6 DRGs. (a) The TNF $\alpha$ -R and IL-1 $\beta$  protein expression levels in the DRG of the gp120 group were increased compared to the sham group ( $p < 0.01$ ). The TNF $\alpha$ -R and IL-1 $\beta$  protein expression levels in the gp120 + RES group were decreased compared to the gp120 group ( $p < 0.01$ ). The expression of IL-10 protein in the DRG of the gp120 group was decreased compared to the sham group ( $p < 0.01$ ). The IL-10 protein expression in the DRG of the gp120 + RES group was increased compared to the gp120 group ( $p < 0.01$ ). (b) The bar histograms show the ratio of TNF $\alpha$ -R, IL-1 $\beta$ , and IL-10 protein levels to the  $\beta$ -actin level in each group. (Note: The data are shown as the mean  $\pm$  SEM. \*\* $p < 0.01$ , compared to the sham group and ## $p < 0.01$ , compared to the gp120 group.)

then reduce the release of cytokines. Inflammatory factors can increase the activation of the P2X<sub>7</sub> receptor, aggravating the neuropathic damage.<sup>34,35</sup> Anti-inflammatory effects could decrease the nociceptive signal of the aggravated DRG neuronal excitation. RES has anti-inflammatory effects.<sup>13–15</sup> Our results suggested that RES relieved the HIV-associated pain behavior in the gp120 rats by influencing the P2X<sub>7</sub> receptor in the DRG SGCs.

P2X receptor-mediated pain transmission is related to ERK signaling.<sup>36</sup> ERK pathway activation participates in the sensitized primary afferents in pain transmission.<sup>37,38</sup> ERK1/2 phosphorylation generates the activation form of ERK1/2. Our data revealed that the IOD ratio of p-ERK1/2 to ERK1/2 was higher in the gp120 group than the sham group. The role of ERK phosphorylation in the DRG may be involved in the P2X<sub>7</sub>

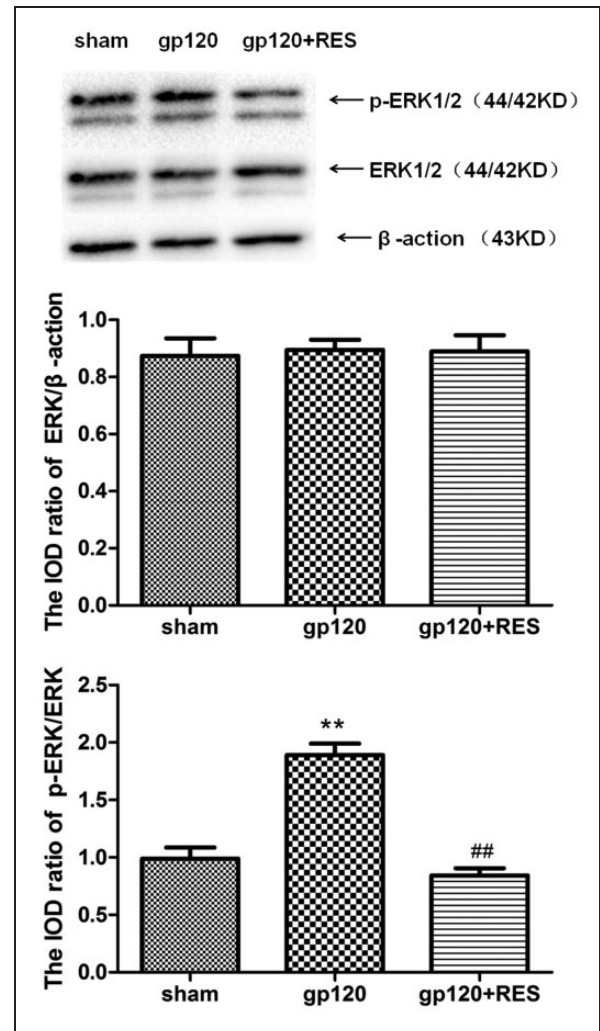


**Figure 5.** Effects of RES on the ERK1/2 and p-ERK1/2 expression levels in L4–6 DRGs. The ERK1/2 and p-ERK1/2 expression levels in the DRG were analyzed using Western blot analysis. The IOD ratio of ERK1/2 to  $\beta$ -actin was not significantly different between the two groups ( $p > 0.05$ ). The IOD ratio of p-ERK1/2 to ERK1/2 in the gp120 group was higher than the sham group ( $n = 6$ ). The IOD ratio of p-ERK1/2 to ERK1/2 in the gp120 + RES-treated rats was significantly lower than that of the gp120 group ( $p < 0.01$ ,  $n = 6$  for each group). The data represent the mean  $\pm$  SEM,  $n = 6$ . \*\* $p < 0.01$  compared to the sham group and ## $p < 0.01$  compared to the gp120 group.

receptor-mediated hyperalgesia in the gp120-treated rats. After the administration of RES, the IOD ratio of p-ERK1/2 to ERK1/2 in the gp120 + RES group was significantly decreased compared with that in the gp120 group. RES may decrease the phosphorylation of ERK1/2 in the DRG of the gp120-treated rats, relieving the P2X<sub>7</sub> receptor-mediated hyperalgesia. To identify whether RES can specially act on the P2X<sub>7</sub> receptor, HEK293 cells that were transfected with the P2X<sub>7</sub> plasmid were evaluated. RES significantly inhibited the

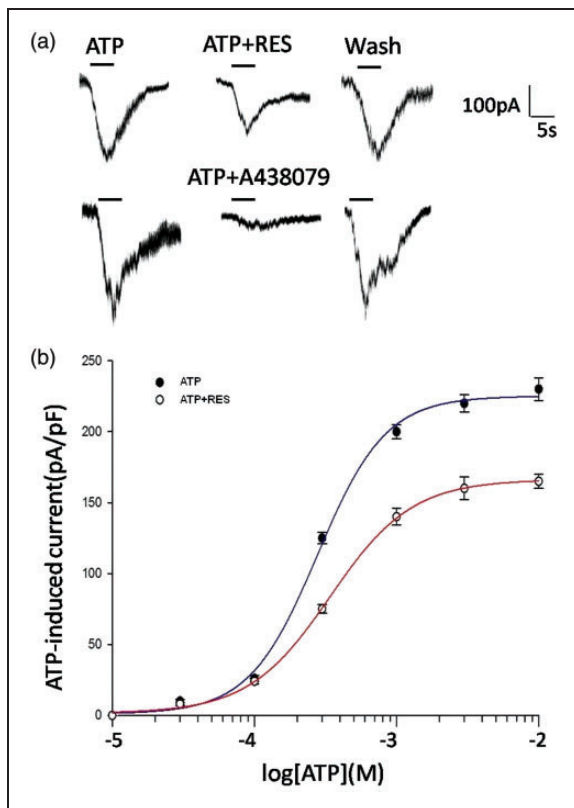


**Figure 6.** Depressive effects of the RES on the ATP-activated current in HEK293 cells transfected with pEGFP-hP2X<sub>7</sub> plasmid. (a) Current traces showed that RES inhibited ATP-activated currents in HEK293 cells expressing the hP2X<sub>7</sub> receptor and the current can be inhibited by specific P2X<sub>7</sub> receptor antagonist A438079. All ATP-activated currents were obtained by application of 10 mM ATP. (b) Concentration dependence of ATP on the peak amplitude of current responses by the P2X<sub>7</sub> receptor in the absence (closed symbols) and presence of RES (100 μM) (open symbols). Data points are the mean ± SEM values from 8 to 10 cells per dose. The EC<sub>50</sub> values in the absence and presence of RES were approximately 270 ± 20 μM and 340 ± 10 μM, respectively.

ATP-activated currents in the HEK293 cells that were transfected with P2X<sub>7</sub> plasmid. These data confirmed that RES relieved the HIV-associated pain behavior in the gp120 rats by acting on the P2X<sub>7</sub> receptor. The electrophysiological data supported the phenomenon, RES treatment relieved the HIV-associated pain behavior relating to downregulation of the P2X<sub>7</sub> receptor expression. In conclusion, the gp120 protein treatment enhanced the expression the P2X<sub>7</sub> receptor in DRG SGCs. The upregulated P2X<sub>7</sub> and GFAP levels in the DRG indicated the activation of SGCs. The activation of SGCs increased the release of inflammatory cytokines (IL-1β and TNF-α) and decreased the release of anti-inflammatory cytokine (IL-10). IL-1β and TNF-α could increase the sensitization of neurons in the DRG, resulting in gp120-induced neuropathic pain behavior. RES dampened the release of inflammatory cytokines,

enhanced the release of an anti-inflammatory cytokine, and reduced the upregulation of the P2X<sub>7</sub> receptor. Inhibition of the P2X<sub>7</sub> receptor in DRG SGCs may decrease the sensitization of neurons in the DRG of the gp120-treated rats. Therefore, RES relieved the mechanical hyperalgesia in the gp120-treated rats relating to inhibition of the P2X<sub>7</sub> receptor in DRG SGCs.

### Author contributions

Bing Wu performed experiments and wrote the manuscript. Bing Wu, Yucheng Ma, Zihua Yi, Shuangmei Liu, Shenqiang Rao, Lifang Zou, Shouyu Wang, Yun Xue, Tianyu Jia, Shanhong Zhao, Lin Li, Huilong Yuan, and Liran Shi performed the experiments. Bing Wu and Shuangmei Liu performed the electrophysiological experiments. Shandong Liang designed the study, supervised the work, wrote, and revised the manuscript. All authors read and approved the final manuscript.

### Declaration of Conflicting Interests

The author(s) declare that there are no potential conflicts of interest with respect to the research, authorship, and/or publication of this article.

### Funding

The author(s) disclose receipt of the following financial support for the research, authorship, and/or publication of this article: This research was supported by the National Natural Science Foundation of China (31560276, 81570735, 81460200, 81171184, 31060139, 30860086, and 81200853), second batch of the Jiangxi Province “Gan Po Excellence Talent 555 project” for talent projects from the Technology Pedestal and Society Development Project of Jiangxi Province (20151122040105), Natural Science Foundation of Jiangxi Province (20142BAB2 05028 and 20142BAB215027), and Educational Department of Jiangxi Province (GJJ13155 and GJJ14319).

### References

- Hao S. The molecular and pharmacological mechanisms of HIV-related neuropathic pain. *Curr Neuropharmacol* 2013; 11: 499–512.
- Parker R, Stein DJ and Jelsma J. Pain in people living with HIV/AIDS: a systematic review. *J Int AIDS Soc* 2014; 17: 18719.
- Schutz SG and Robinson-Papp J. HIV-related neuropathy: current perspectives. *HIV AIDS (Auckl)* 2013; 5: 243–251.
- Hoke A, Morris M and Haughey NJ. GPI-1046 protects dorsal root ganglia from gp120-induced axonal injury by modulating store-operated calcium entry. *J Peripher Nerv Syst* 2009; 14: 27–35.
- Yuan SB, Shi Y, Chen J, et al. Gp120 in the pathogenesis of human immunodeficiency virus-associated pain. *Ann Neurol* 2014; 75: 837–850.
- Maratou K, Wallace VC, Hasnie FS, et al. Comparison of dorsal root ganglion gene expression in rat models of traumatic and HIV-associated neuropathic pain. *Eur J Pain* 2009; 13: 387–398.



7. Nasirinezhad F, Jergova S, Pearson JP, et al. Attenuation of persistent pain-related behavior by fatty acid amide hydrolase (FAAH) inhibitors in a rat model of HIV sensory neuropathy. *Neuropharmacology* 2015; 95: 100–109.
8. Zheng W, Ouyang H, Zheng X, et al. Glial TNF $\alpha$  in the spinal cord regulates neuropathic pain induced by HIV gp120 application in rats. *Mol Pain* 2011; 7: 40.
9. Phillips TJ, Brown M, Ramirez JD, et al. Sensory, psychological, and metabolic dysfunction in HIV-associated peripheral neuropathy: A cross-sectional deep profiling study. *Pain* 2014; 155: 1846–1860.
10. Chi X, Amet T, Byrd D, et al. Direct effects of HIV-1 Tat on excitability and survival of primary dorsal root ganglion neurons: possible contribution to HIV-1-associated pain. *PLoS One* 2011; 6: e24412.
11. Basbaum AI, Bautista DM, Scherrer G, et al. Cellular and molecular mechanisms of pain. *Cell* 2009; 139: 267–284.
12. Mangus LM, Dorsey JL, Laast VA, et al. Unraveling the pathogenesis of HIV peripheral neuropathy: insights from a simian immunodeficiency virus macaque model. *ILAR J* 2014; 54: 296–303.
13. Shimazu Y, Shibuya E, Takehana S, et al. Local administration of resveratrol inhibits excitability of nociceptive wide-dynamic range neurons in rat trigeminal spinal nucleus caudalis. *Brain Res Bull* 2016; 124: 262–268.
14. Steiner N, Balez R, Karunaweera N, et al. Neuroprotection of Neuro2a cells and the cytokine suppressive and anti-inflammatory mode of action of resveratrol in activated RAW264.7 macrophages and C8-B4 microglia. *Neurochem Int* 2016; 95: 46–54.
15. Takehana S, Sekiguchi K, Inoue M, et al. Systemic administration of resveratrol suppress the nociceptive neuronal activity of spinal trigeminal nucleus caudalis in rats. *Brain Res Bull* 2016; 120: 117–122.
16. Burnstock G. Purinergic receptors and pain. *Curr Pharm Des* 2009; 15: 1717–1735.
17. Burnstock G. Purinergic mechanisms and pain—an update. *Eur J Pharmacol* 2013; 716: 24–40.
18. Chizh BA and Illes P. P2X receptors and nociception. *Pharmacol Rev* 2001; 53: 553–568.
19. Skaper SD, Debetto P and Giusti P. The P2X7 purinergic receptor: from physiology to neurological disorders. *FASEB J* 2010; 24: 337–345.
20. Sperlagh B, Vizi ES, Wirkner K, et al. P2X7 receptors in the nervous system. *Prog Neurobiol* 2006; 78: 327–346.
21. Hazleton JE, Berman JW and Eugenin EA. Purinergic receptors are required for HIV-1 infection of primary human macrophages. *J Immunol* 2012; 188: 4488–4495.
22. Lee BH, Hwang DM, Palaniyar N, et al. Activation of P2X(7) receptor by ATP plays an important role in regulating inflammatory responses during acute viral infection. *PLoS One* 2012; 7: e35812.
23. Wallace VC, Blackbeard J, Pheby T, et al. Pharmacological, behavioural and mechanistic analysis of HIV-1 gp120 induced painful neuropathy. *Pain* 2007; 133: 47–63.
24. Friedman LK, Goldstein B, Rafiuddin A, et al. Lack of resveratrol neuroprotection in developing rats treated with kainic acid. *Neuroscience* 2013; 230: 39–49.
25. Lin J, Li G, Den X, et al. VEGF and its receptor-2 involved in neuropathic pain transmission mediated by P2X(2)/(3) receptor of primary sensory neurons. *Brain Res Bull* 2010; 83: 284–291.
26. Zhang Z, Liu X, Lu S, et al. Increased pain in response to mechanical or thermal stimulation in a rat model of incision-induced pain with nicotine dependence and withdrawal. *Exp Ther Med* 2013; 5: 1063–1066.
27. Tu G, Li G, Peng H, et al. P2X(7) inhibition in stellate ganglia prevents the increased sympathoexcitatory reflex via sensory-sympathetic coupling induced by myocardial ischemic injury. *Brain Res Bull* 2013; 96: 71–85.
28. Liu S, Zou L, Xie J, et al. LncRNA NONRATT021972 siRNA regulates neuropathic pain behaviors in type 2 diabetic rats through the P2X7 receptor in dorsal root ganglia. *Mol Brain* 2016; 9(1): 44.
29. Herzberg U and Sagen J. Peripheral nerve exposure to HIV viral envelope protein gp120 induces neuropathic pain and spinal gliosis. *J Neuroimmunol* 2001; 116: 29–39.
30. Mehta N, Kaur M, Singh M, et al. Purinergic receptor P2X(7): a novel target for anti-inflammatory therapy. *Bioorg Med Chem* 2014; 22: 54–88.
31. Hanani M. Satellite glial cells in sensory ganglia: from form to function. *Brain Res Brain Res Rev* 2005; 48: 457–476.
32. Dublin P and Hanani M. Satellite glial cells in sensory ganglia: their possible contribution to inflammatory pain. *Brain Behav Immun* 2007; 21: 592–598.
33. Blum E, Procacci P, Conte V, et al. Systemic inflammation alters satellite glial cell function and structure. A possible contribution to pain. *Neuroscience* 2014; 274: 209–217.
34. Kushnir R, Cherkas PS and Hanani M. Peripheral inflammation upregulates P2X receptor expression in satellite glial cells of mouse trigeminal ganglia: a calcium imaging study. *Neuropharmacology* 2011; 61: 739–746.
35. Old EA and Malcangio M. Chemokine mediated neuron-glia communication and aberrant signalling in neuropathic pain states. *Curr Opin Pharmacol* 2012; 12: 67–73.
36. Seino D, Tokunaga A, Tachibana T, et al. The role of ERK signaling and the P2X receptor on mechanical pain evoked by movement of inflamed knee joint. *Pain* 2006; 123: 193–203.
37. Ji RR, Gereau RT, Malcangio M, et al. MAP kinase and pain. *Brain Res Rev* 2009; 60: 135–148.
38. Lai HH, Qiu CS, Crock LW, et al. Activation of spinal extracellular signal-regulated kinases (ERK) 1/2 is associated with the development of visceral hyperalgesia of the bladder. *Pain* 2011; 152: 2117–2124.